ISSN 1070-3284, Russian Journal of Coordination Chemistry, 2019, Vol. 45, No. 5, pp. 356–360. © Pleiades Publishing, Ltd., 2019.
Russian Text © The Author(s), 2019, published in Koordinatsionnaya Khimiya, 2019, Vol. 45, No. 5, pp. 306–310.

Polynuclear Glycinehydroximate Cu(II)–Gd(III) Metallamacrocyclic Complexes: Halochromic Properties

G. Yu. Zhigulin[a], *, G. S. Zabrodina[a], M. A. Katkova[a], and S. Yu. Ketkov[a]

[a] *Razuvaev Institute of Organometallic Chemistry, Russian Academy of Sciences, Nizhny Novgorod, 603950 Russia*

**e-mail: gzhigulin@gmail.com*

Received July 6, 2018; revised October 24, 2018; accepted December 3, 2018

Abstract—It was shown by electronic spectroscopy that the visible absorption spectrum of the polynuclear Cu(II)–Gd(III) metallamacrocyclic complex is pH-sensitive. The intensity of the absorption peak at 577 nm decreases 5-fold as the pH decreases from 6.8 to 3.3 and restores the initial level as the pH increases up to 12.4. On the basis of DFT calculations and analysis of topological electron density characteristics, the spectral changes were attributed to protonation of the glycinehydroximate ligand.

Keywords: polynuclear metallamacrocyclic complexes, Cu(II), Gd(III), halochromism, DFT calculations

DOI: 10.1134/S107032841905004X

INTRODUCTION

Polynuclear metallamacrocyclic compounds, which were first described by an American research team headed by Pecoraro in 1989, represent a unique class of supramolecular compounds structurally resembling crown ethers [1–3]. Our research addresses water-soluble *d–f*-polynuclear 15-MC-5 metallacrowns based on α-amino hydroxamic acids [4]. α-Amino hydroxamic acids (NH_2–CHR–CO–NH–OH), which are known for the broad spectrum of biological activity, are efficient N,N- and O,O-type chelating ligands. A distinctive feature of the chelate complexes based on hydroxamic acids is the diversity of the resulting structures depending on the substituent R and the nature of the metal, which can be used to model a number of natural enzymes [5, 6]. It is noteworthy that change in the pH is a simple internal stimulus inducing the "on–off–on" of the enzyme action [7]. The halochromism phenomenon is related to the reversible change in the absorption spectrum depending on the pH. However, most of known halochromic compounds are based on organic molecules, while metal complexes receive much less attention [8]. Among transition metal complexes, copper(II) compounds are considered to be most promising for the development of chemically pH-sensitive materials [9]. Previously, we developed an original synthetic approach to water-soluble heteronuclear copper(II) and lanthanide(III) 15-MC-5 complexes based on glycine hydroxamic acid [10–14]. The Cu(II) and Gd(III) complexes are of their own interest as regards their use as contrast agents for high-field MRI [15, 16]. As a continuation of these works, in order to elucidate the behavior of polynuclear metallamacrocycle at various pH, we studied the halochromic properties of 15-MC-5 derivatives associated with the protonation of the aminohydroximate nitrogen atom for a Cu(II)–Gd(III) glycinehydroximate complex.

EXPERIMENTAL

Commercial (Aldrich) copper acetate monohydrate, gadolinium chloride hexahydrate, and glycine hydroxamic acid were used.

Synthesis of $Gd(H_2O)_4[15\text{-}MC_{Cu(II)Glyha}\text{-}5](Cl)_3 \cdot 10H_2O$ (I). Glycine hydroxamic acid (0.09 g, 1 mmol) was added with vigorous stirring to a solution of $Cu(OAc)_2 \cdot H_2O$ (0.2 g, 1 mmol) and $GdCl_3 \cdot 6H_2O$ (0.08 g, 0.2 mmol) in doubly distilled water (25 mL). After 40 min, the solution acquired a deep blue-violet color. The mixture was kept for 24 h at 20°C and filtered. The dark blue needle crystals were prepared by slow evaporation of the aqueous filtrate at 40°C and twice recrystallized from water. The yield was 0.21 g (84%).

For $C_{10}H_{48}Cl_3Cu_5GdN_{10}O_{24}$

Anal. calcd., %	C, 9.43	H, 3.80	N, 11.00	Gd, 12.34
Found, %	C, 9.41	H, 3.83	N, 11.03	Gd, 12.29

IR (ν, cm^{-1}): 3220 w, 1642 m, 1594 s, 1439 m, 1403 m, 1308 m, 1177 w, 1147 w, 1135 w, 1074 s, 1035 s, 933 w, 602 w, 545 w, 488 m. UV (293 K, H_2O): λ = 575 nm.

IR spectra were measured on an FSM 1201 Fourier transform IR spectrometer. The sample was prepared by a standard procedure in mineral oil. The electronic

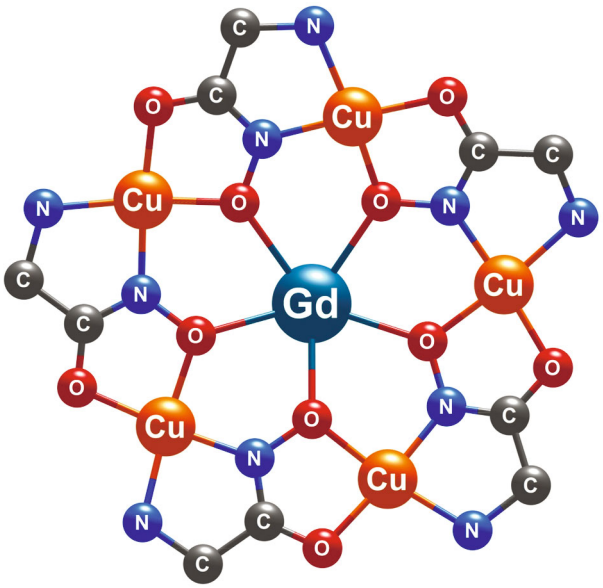

Fig. 1. Structure of complex **I** (hydrogen atoms and water molecules are omitted).

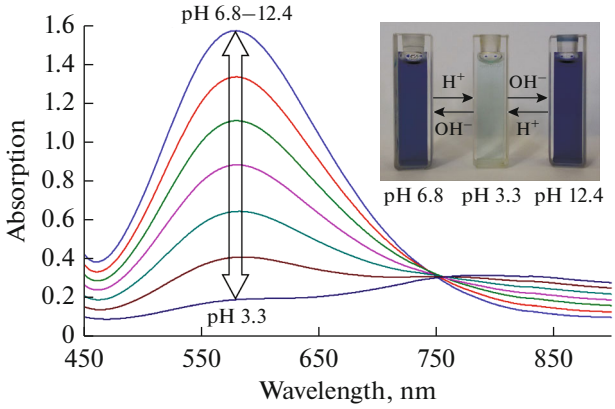

Fig. 2. Electronic spectrum of complex **I** as a function of pH.

absorption spectra were measured on a Perkin Elmer Lambda 25 spectrometer. Elemental analysis was performed using a Euro EA 3000 C,H,N analyzer.

Calculation procedure. The DFT study of model copper-containing 15-MC-5 moieties was implemented using the Gaussian09 program package [17]. The geometry was optimized using the hybrid B3LYP XC functional [18–20] and the DGDZVP double ζ-basis set [21, 22] in the polarized continuum model (PCM) [23] to take into account the solvent (water). The energy minima of the structures obtained upon optimization were confirmed by analysis of harmonic vibrations, among which no imaginary frequency modes were present. The trinuclear copper(II) complexes with overall charges of +2 and +3 were modeled as high-spin systems with a multiplicity of 4. The deformation electron density maps were derived using the Multiwfn 3.3.9 program [24] by subtracting the electron density of spherically symmetrical atoms from the molecular electron density of the complexes. Atoms-in-molecules (QTAIM) analysis [25, 26] was performed using the AIMAll program [27].

RESULTS AND DISCUSSION

The water-soluble complex $Gd(H_2O)_4[15\text{-}MC_{Cu(II)Glyha}\text{-}5](Cl)_3$ (**I**) was synthesized in air at room temperature from glycinehydroxamic acid, copper(II) acetate, and Gd(III) chloride. A specific structural feature of complex **I** is the presence of a planar metallamacrocycle consisting of five Cu^{2+} ions, five glycinehydroximate ligands, and the central Gd^{3+} ion, which is coordinated to five oxygen atoms of the metallamacrocycle [15] (Fig. 1). Apart from the ligand oxygen atoms, the gadolinium coordination sphere contains four water molecules.

This metallamacrocyclic structure of the copper "crown" gives rise to a typical electronic spectrum with a band at 577 nm (ε = 420 M^{-1} cm^{-1}) corresponding to Cu(II) *d–d* transitions. Complex **I** was found to possess halochromic properties. Indeed, the intensity of the 577 nm peak declines 5-fold on treatment with acids, as the pH decreases from 6.8 to 3.3, and is then restored upon the addition of a base, as the pH increases to 12.4 (Fig. 2).

The observed pH-induced change in the signal intensity can be attributed to the reversible change of the chromophore structure upon protonation and deprotonation of hydroximate ligands of the metallamacrocyclic ring. Oxyamide groups are known to exist as diverse isomers and tautomers, which accounts for them being called "chemical chameleons" [28]. The DFT quantum chemical calculations at the B3LYP/DGDZVP level demonstrated that protonation of the imine nitrogen N(1) in model moiety A of the metallamacrocycle increases the deformation electron density (DED) along the Cu–N(1) bond in the vicinity of nitrogen (Fig. 3). It is of interest that the charge on the nitrogen atom becomes less negative (the charge calculated in terms of QTAIM varies from –0.68 to –0.59 e). Upon protonation, the Cu–N(1) distance increases from 1.961 to 2.231 Å; the other coordination bonds of copper vary insignificantly (Table 1).

The QTAIM studies predict a considerable decrease in the electron density $\rho(\mathbf{r})$ and the Laplacian $\nabla^2\rho(\mathbf{r})$ at the (3, –1) critical point of the Cu–N(1) bond, from 0.0981 to 0.0535 a.u. and from 0.3038 to 0.1700 a.u., respectively (Table 2). It has been found [29] for Cu(II) complexes that the $\rho(\mathbf{r})$ and $\nabla^2\rho(\mathbf{r})$ values at the (3, –1) critical point decrease in a similar way upon elongation of the coordination bond, which is accompanied by an increase in the positive DED maximum in the vicinity of the donor atom. The ratio

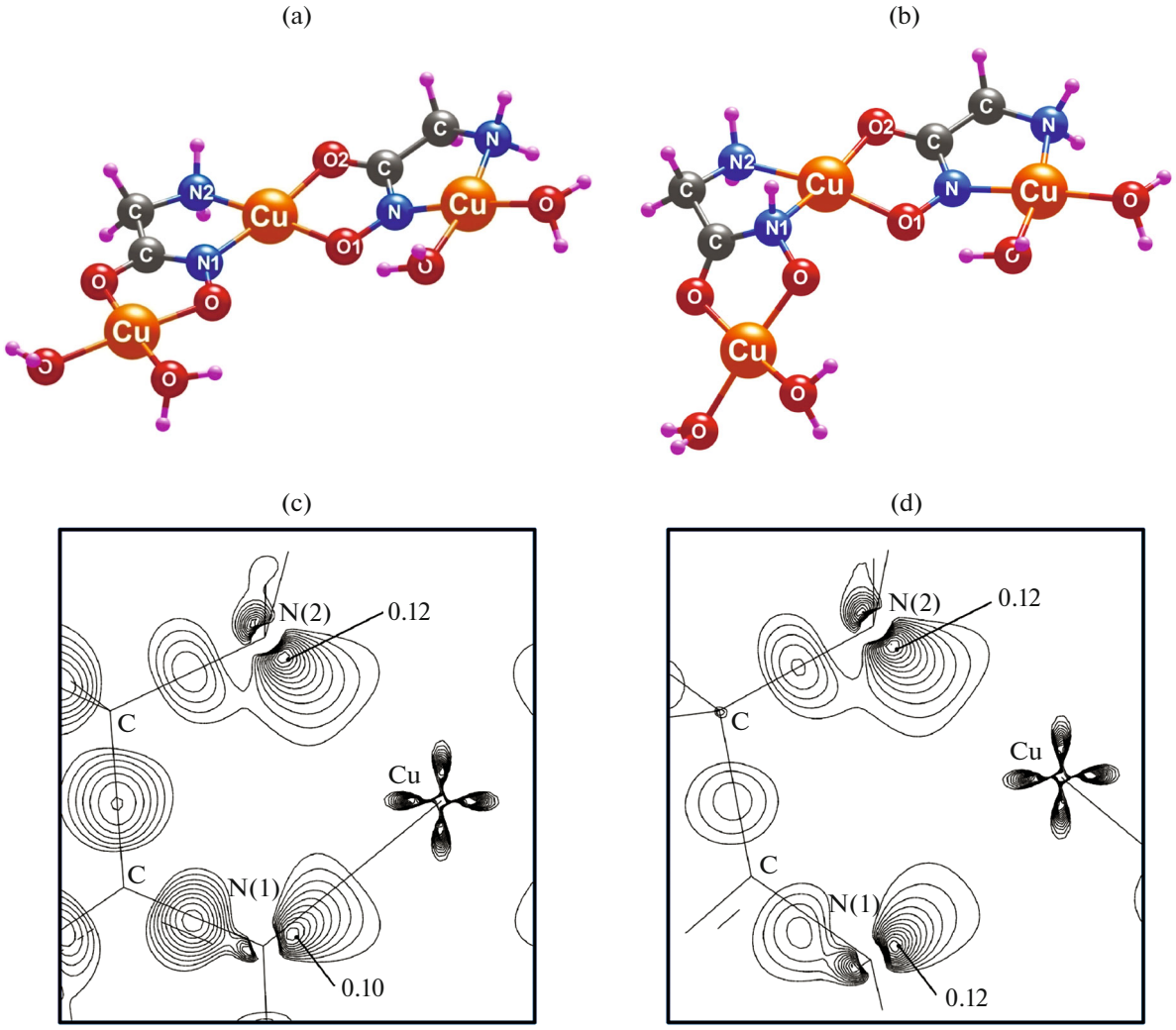

Fig. 3. Optimized structures of model moieties (a) A and (b) B of complex **I** and (c, d) corresponding positive deformation electron density maps (0.01–0.13 a.u., with a 0.01 a.u. step.) in the CuN(1)N(2) planes.

of the modulus of potential energy density $|V(\mathbf{r})|$ to the kinetic energy density $G(\mathbf{r})$ serves to classify the interatomic contacts: $|V(\mathbf{r})|/G(\mathbf{r}) < 1$ attests to closed-shell interaction, in particular, ionic one, while $|V(\mathbf{r})|/G(\mathbf{r}) > 2$ is inherent in covalent bonds [30, 31]. The calculated $|V(\mathbf{r})|/G(\mathbf{r})$ values at the critical points of the copper coordination bonds with the glycinehydroximate ligands occur in the range from 1 to 2 (Table 2), which corresponds to an intermediate type of interactions. Note that the decrease in the $|V(\mathbf{r})|/G(\mathbf{r})$ value of the

Table 1. Interatomic distances (Å) of complex **I** according to X-ray diffraction data [15] and model moieties A and B according to DFT data

Bond	*d*, Å		
	I	A*	B*
$Cu–N_{imine}$	1.905(3)–1.929(3)	1.961	2.231
$Cu–N_{amine}$	2.005(4)–2.023(3)	2.056	2.040
$Cu–O_{oxime}$	1.928(3)–1.944(3)	1.965	1.921
$Cu–O_{carbonyl}$	1.946(3)–1.957(3)	1.990	1.993

* Distances to the central copper atom.

Table 2. Topological parameters of the electron density (a.u.) at the (3, −1) critical points of the coordination bonds of the central copper atom of model moieties A and B

Atoms	$\rho(\mathbf{r})$	$\nabla^2\rho(\mathbf{r})$	$V(\mathbf{r})$	$G(\mathbf{r})$	$\lvert V(\mathbf{r})\rvert/G(\mathbf{r})$
			A		
Cu–N(1)	0.0981	0.3038	−0.1764	0.1262	1.3978
Cu–N(2)	0.0821	0.2278	−0.1361	0.0965	1.4104
Cu–O(1)	0.0892	0.3333	−0.1692	0.1262	1.3407
Cu–O(2)	0.0830	0.3203	−0.1569	0.1185	1.3241
			B		
Cu–N(1)	0.0535	0.1700	−0.0754	0.0590	1.2780
Cu–N(2)	0.0840	0.2472	−0.1434	0.1026	1.3977
Cu–O(1)	0.0992	0.3757	−0.1929	0.1434	1.3452
Cu–O(2)	0.0840	0.3099	−0.1567	0.1171	1.3382

Cu–N(1) bond from 1.3978 to 1.2780 upon protonation (A → B) does not change the bond nature, although attests to increasing ionic contribution. Previously, it was shown that the potential energy density at the (3, −1) critical point is correlated with the coordination bond energy [32, 33]. Therefore, the decrease in the $|V(\mathbf{r})|$ value from 0.1764 to 0.0754 (Table 2) may be taken as pointing to a considerable weakening of the Cu–N(1) bond upon protonation.

Analysis of the molecular orbitals of model complexes A and B demonstrated that the addition of a proton to nitrogen decreases the energy gap between the β-HOMO and β-LUMO from 1.91 to 1.53 eV. The difference between the β-LUMO and β-HOMO energies of moiety A containing contributions of copper *d* orbitals is in good agreement with the observed position of the absorption maximum in the electronic spectrum of **I**, which corresponds to an energy of 2.15 eV. The calculated decrease in the β-HOMO—β-LUMO gap upon protonation of A corresponds to the shift of the electron transition to 800 nm. Indeed, a decrease in the pH leads to increasing absorption in the long-wavelength spectral range (Fig. 2). Thus, the calculations confirm that the color change of a solution of complex **I** is attributable to protonation of hydroximate ligand nitrogen.

ACKNOWLEDGMENTS

The measurements were performed using the equipment of the Center for Collective Use Analytical Center of the IOMC RAS.

FUNDING

The studies of electron density and spectral properties of the complexes were supported by the Russian Science Foundation (project no. 18-13-00356). G.Yu. Zhigulin is grateful to the support from the Russian Foundation for Basic Research (project no. 18-33-01252 mol_a).

REFERENCES

1. Mezei, G., Zaleski, C.M., and Pecoraro, V.L., *Chem. Rev.*, 2007, vol. 107, p. 4933.
2. Tegoni, M. and Remelli, M., *Coord. Chem. Rev.*, 2012, vol. 256, p. 289.
3. Bodwin, J.J., Cutland, A.D., Malkani, R.G., et al., *Coord. Chem. Rev.*, 2001, vols. 216–217, p. 489.
4. Katkova, M.A., *Russ. J. Coord. Chem.*, 2018, vol. 44, p. 284. doi 10.1134/S107032841804005X
5. Sigel, H. and Martin, R.B., *Chem. Rev.*, 1982, vol. 82, p. 385.
6. Ford, P., *Chem. Sci.*, 2016, vol. 7, p. 2964.
7. Guha, S., Liu, J., Baltazar, G., et al., *Adv. Exp. Med. Biol.*, 2014, vol. 801, p. 105.
8. Solomon, E.I., Heppner, D.E., Johnston, E.M., et al., *Chem. Rev.*, 2014, vol. 114, p. 3659.
9. Golchoubian, H., Moayyedi, G., Rezaee, E., et al., *Polyhedron*, 2015, vol. 96, p. 71.
10. Katkova, M.A., Zabrodina, G.S., Muravyeva, M.S., et al., *Inorg. Chem. Commun.*, 2015, vol. 52, p. 31.
11. Katkova, M.A., Zabrodina, G.S., Muravyeva, M.S., et al., *Eur. J. Inorg. Chem.*, 2015, vol. 2015, p. 5202.
12. Kremlev, K.V., Samsonov, M.A., Zabrodina, G.S., et al., *Polyhedron*, 2016, vol. 114, p. 96.
13. Makarov, S.G., Zabrodina, G.S., Cherkasov, A.V., et al., *Macroheterocycles*, 2016, vol. 9, p. 263.
14. Katkova, M.A., Zabrodina, G.S., Kremlev, K.V., et al., *Thin Solid Films*, 2017, vol. 628, p. 112.
15. Muravyeva, M.S., Zabrodina, G.S., Samsonov, M.A., et al., *Polyhedron*, 2016, vol. 114, p. 165.
16. Katkova, M.A., Zabrodina, G.S., Baranov, E.V., et al., *Appl. Organomet. Chem.*, 2018, vol. 32. e4389. doi 10.1002/aoc.4389
17. Frisch, M.J., Trucks, G.W., Schlegel, H.B., et al., *Gaussian 09, Revision B.01*, Wallingford: Gaussian, Inc., 2010.
18. Becke, A.D., *J. Chem. Phys.*, 1993, vol. 98, p. 5648.
19. Lee, C., Yang, W., and Parr, R.G., *Phys. Rev. B: Condens. Matter.*, 1988, vol. 37, p. 785.

20. Stephens, P.J., Devlin, F.J., Chabalowski, C.F., et al., *J. Phys. Chem.*, 1994, vol. 98, p. 11623.
21. Godbout, N., Salahub, D.R., Andzelm, J., et al., *Can. J. Chem.*, 1992, vol. 70, p. 560.
22. Sosa, C., Andzelm, J., Elkin, B.C., et al., *J. Phys. Chem.*, 1992, vol. 96, p. 6630.
23. Tomasi, J., Mennucci, B., and Cammi, R., *Chem. Rev.*, 2005, vol. 105, p. 2999.
24. Lu, T. and Chen, F., *J. Comput. Chem.*, 2012, vol. 33, p. 580.
25. Bader, R.F.W., *Atoms in Molecules: A Quantum Theory*, Oxford: Oxford Univ., 1990.
26. Cortes-Guzman, F. and Bader, R.F.W., *Coord. Chem. Rev.*, 2005, vol. 249, p. 633.
27. Keith, T.A., AIMAll. Version 10.05.04. Overland Park: TK Gristmill Software, 2010. http://aim.tkgristmill.com.
28. Mikhaleva, A.I., Zaitsev, A.B., and Trofimov, B.A., *Russ. Chem. Rev.*, 2006, vol. 75, p. 797.
29. Dos Santos, L.H.R., Lanza, A., Barton, A.M., et al., *J. Am. Chem. Soc.*, 2016, vol. 138, p. 2280.
30. Espinosa, E., Alkorta, I., Elguero, J., et al., *J. Chem. Phys.*, 2002, vol. 117, p. 5529.
31. Gibbs, G.V., Cox, D.F., Crawford, T.D., et al., *J. Chem. Phys.*, 2006, vol. 124, p. 084704.
32. Borissova, A.O., Korlyukov, A.A., Antipin, M.Yu., and Lyssenko, K.A., *J. Phys. Chem. A*, 2008, vol. 112, p. 11519.
33. Puntus, L.N., Lyssenko, K.A., Antipin, M.Yu., and Bunzli, J.-C.G., *Inorg. Chem.*, 2008, vol. 47, p. 11095.

Translated by Z. Svitanko